



ACADEMIC
PRESS

Available online at www.sciencedirect.com

SCIENCE @ DIRECT®

Journal of Magnetic Resonance 159 (2002) 13–24

JMR

Journal of
Magnetic Resonance

www.academicpress.com

PFG NMR measurements of flow through porous media: effects of spatial correlations of the magnetic field and the velocity field

L. Lebon* and J. Leblond

Laboratoire de Physique et Mécanique des Milieux Hétérogènes, UMR 7636 CNRS, ESPCI 10 rue Vauquelin, 75231 Paris cedex 05, France

Received 27 February 2002; revised 15 July 2002

Abstract

Used for a long time for diffusion studies, PFG NMR techniques are now widely used to study flow through porous media. We discuss here the effects of the magnetic field inhomogeneities and the finite gradient pulse duration in this case. We propose a statistical model based on spatial correlations of the magnetic field and velocity field and as far as we can, we draw practical conclusions on the PFG NMR measurements conditions.

© 2002 Elsevier Science (USA). All rights reserved.

1. Introduction

For a long time, there has been an important interest in the use of NMR (nuclear magnetic resonance) to investigate porous media. Different NMR techniques such as relaxation measurements [1–4], NMR imaging [5,6] (MRI) or PFG NMR (pulsed-field-gradient NMR) have been used to characterise geometrical properties or dynamics of fluid phases through the porous media. PFG NMR appears to be particularly interesting, since it allows fluid transport characterisation with a spatial resolution higher than what can be achieved by MRI; this technique was thoroughly used to investigate diffusion processes [7–11], but flow studies in porous media have also been reported [12–18].

The key point in PFG NMR techniques is the fact that, theoretically, the magnetisation decay $M_{\Delta}(k)$ as a function of the pulsed field gradient intensity is directly the Fourier transform of the averaged propagator $P_{\Delta}(\xi)$:

$$M_{\Delta}(k) = M_0 \int P_{\Delta}(\xi) e^{ik\xi} d\xi \quad (1)$$

where $M_{\Delta}(k)$ is the echo magnetisation, Δ is the time interval between gradient pulses, and k is the reciprocal length: $k = \gamma g \delta$ where γ is the gyromagnetic ratio, g is the pulsed gradient intensity, and δ is the pulsed gradient duration. As introduced by Callaghan [19], the av-

eraged propagator $P_{\Delta}(\xi)$ is the probability distribution of displacement ξ along the direction of the pulsed gradient over a time Δ . This function allows one to determine all the statistics of fluid transport through the porous media and it is particularly relevant for the study of complex transport processes.

More generally, Eq. (1) derives from the the total dephasing $\varphi = \phi(\Delta)$ accumulated by each fluid particle when it flows through the porous medium during the time interval Δ . The magnetisation decay results from the ensemble average over all the particle dephasing:

$$M_{\Delta} = M_0 \int p(\varphi) e^{i\varphi} d\varphi, \quad (2)$$

where $p(\varphi)$ is the probability distribution of dephasing. Let us remark that, in this case, we neglect any relaxation effects. To study dynamics, the pulsed NMR sequences used for PFG NMR measurements are designed so that the dephasing induced by the applied gradient pulses is:

$$\varphi_a = k\xi. \quad (3)$$

So, it is clear that the propagator is easily determined if the total dephasing is only φ_a or if the other dephasing terms can be neglected (in this case, while $\varphi = \varphi_a$, Eqs. (2) and (3) straightforwardly give Eq. (1)).

Unfortunately, in some cases, the relation between total dephasing and displacement is not as simple as this previous linear equation: there are perturbing effects like internal field inhomogeneities (for a porous medium,

* Corresponding author. Fax: +1-40-79-44-25.

E-mail address: lebon@pmmh.espci.fr (L. Lebon).

this is due to the difference between the magnetic susceptibility of the grain and that of the fluid) or the finite duration of each gradient pulse. The effects of field inhomogeneities are a constant problem for the use of NMR in porous media and particularly for PFG NMR techniques: when a fluid particle will travel through the porous medium, it will accumulate an uncertain dephasing depending on its trajectory through the sample. Let us call $b(\vec{r})$ the fluctuating part of the magnetic field: $b(\vec{r}) = B(\vec{r}) - B_0$, where $B(\vec{r})$ is the local magnetic field and $B_0 = \langle B(\vec{r}) \rangle$. For a travel time T , the dephasing induced by internal field inhomogeneities is, for each fluid particle:

$$\varphi_b = \int_0^T \gamma b[\vec{r}(t)] dt. \quad (4)$$

The total dephasing is therefore $\varphi = \varphi_a + \varphi_b$; Eq. (1) is no longer valid and the determination of the propagator becomes problematic. We can remark that the latter term (φ_b) arises, even in the absence of any applied gradient pulse.

In its general formulation, the problem becomes very difficult to deal with: first, fluid dynamics process ($\vec{r}(t)$) and magnetic properties ($b(\vec{r})$) are coupled. And second, the knowledge of magnetic field spatial distribution requires the solution of the Maxwell equations with the correct boundary conditions: it turns out to be impossible for any arbitrary random porous matrix, and even for modeled porous media such as monodisperse sphere packing, this is not obvious. So, in the absence of a general theory for transport in an inhomogeneous field, different approximate approaches have been introduced to deal with such a problem, mostly in the case of diffusion in an inhomogeneous field.

Very early, the approximation of a uniform background gradient g_0 has been introduced as an attempt to describe inhomogeneities. For free diffusion in an unrestricted medium, Hahn [20] (by using a random walk model) or Torrey [21] (by introducing a diffusion term in Bloch equations) obtained the same expression for the magnetisation decay. It is clear that such an approximation is very crude to describe diffusion in a porous medium: the linearisation of internal field inhomogeneities can only be valid for very short times (i.e., corresponding to fluid displacements much smaller than the pore size) and wall effects were not taken into account.

To extend this attempt, the Gaussian-phase approximation has been introduced, assuming that the probability distribution of net dephasing φ is Gaussian. Using this approximation, different authors have considered wall effects ([22], for simple pore geometries and uniform gradient) or general inhomogeneous field [23]. As pointed out by some authors [23–25], such an approximation has a restricted validity range and, in practice, it holds for short times and is exact for all times for a uniform gradient in an unbounded medium.

Now, more sophisticated approaches used to describe diffusion in inhomogeneous field have been introduced. As an extension to the constant and uniform gradient g_0 , Le Doussal and Sen [25] have presented an analytic solution to the problem of diffusion in a parabolic magnetic field. They find characteristic length and time scales for such a problem and they obtained scaling laws in agreement with experimental data in porous media. Another way to deal with such a question is to consider spatial correlation of the inhomogeneous magnetic field. For instance, Brown and Fantazzini [26] obtained results in qualitative agreement with experiments. Some theoretical works have also been published for the problem of spins diffusing in a random field [27,28].

This paper is devoted to the presentation of a statistical model which describes the effects of internal field inhomogeneities on PFG NMR experiment of flows through a random porous medium; it is based on the spatial correlation of the magnetic field. We introduce this model because the description of magnetic field inhomogeneities by background gradients cannot be used in the flow case; this is a local description of inhomogeneities and can be used only for small enough displacements. Background gradient description could therefore be adequate for diffusion processes, but it is not for flow processes.

The effects of the gradient pulses' finite duration are also discussed. Such effects are easily taken into account for free diffusion, but in the case of restricted diffusion the theory is not fixed. In the flow case, a simple expansion shows that, during the gradient pulse, we also encode the fluid particle velocities in addition to their positions.

We first present the phase shift induced by the magnetic field inhomogeneities and the velocity variations, and thus, we obtain an expression for the magnetisation decay in the most general case (Section 2). In Section 3, we introduce a statistical model based on the spatial correlations of the magnetic field and the velocity field. After this general discussion, we try, to the extent possible, to draw practical conclusions from this study. In Section 4, we present the application of our results to porous media that are not too pathological (typically those for which it is possible to define a unique length scale l_c , the grain size corresponding to the grain diameter for monodisperse bead pack). Finally, in Section 5, we discuss quantitatively such effects using the parameters from the PFG NMR experiments we previously performed.

2. Magnetisation decay at echo time for PFG NMR

Let us consider the case of a fluid particle flowing through a porous medium. Here, the behaviour of each particle is determined: the flow is assumed to be sta-

tionary and laminar and we neglect molecular diffusion effects. In those conditions, each particle j follows a given trajectory T_j that could be known by solving the transport equations in the appropriate medium. In that case, along the trajectory T_j of the fluid particle j , $b(\vec{r})$ is a function of the particle position along Oz , the direction of the mean flow; neglecting back flow

$$b(\vec{r})_{\text{along } T_j} = b_j(z). \quad (5)$$

In a very similar way, at each position \vec{r} in the fluid, we introduce $v(\vec{r})$ the deviation of the z -component of the fluid velocity defined as $v(\vec{r}) = v_z(\vec{r}) - \langle v_z(\vec{r}) \rangle$, where $v_z(\vec{r})$ is the z -component of the fluid velocity at the position \vec{r} and $\langle \dots \rangle$ represents an ensemble average on all the fluid particles in the porous medium. Note that

$$\langle v_z(\vec{r}) \rangle = U = Q/(S\phi) \quad (Q \text{ is the global flow rate, } \phi \text{ and } S \text{ are the sample porosity and cross-section}).$$

Along the trajectory T_j of the particle j , $v(\vec{r})$, like $b(\vec{r})$, is a function of the position z along the axis Oz ; neglecting back flow

$$v(\vec{r})_{\text{along } T_j} = v_j(z). \quad (6)$$

We consider the general expression (Eq. (2)) for the magnetisation decay that can be simply expressed as $M(k) = M_0 \langle e^{i\Delta\phi_j} \rangle_j$. The first step is to give an expression for $\Delta\phi_j$, the total dephasing at echo time for each particle j . While it depends on the PFG NMR sequence used, we will discuss first the case of the PFG-SE sequence [29] and the PFG-SSE sequence [30], the third one (the APFG-SSE sequence [31], the alternating PFG-SSE sequence) will be examined later. Fig. 1 displays the sequences used in this paper. Here, the time interval τ remains short enough so that fluid displacements during τ are much smaller than typical pore size.¹ This condition allows us to make the assumption that, for each fluid particle, $b(z)$ and $v(z)$ are constant during the time interval τ .

The first term, $\Delta\phi_b$, which arises in the total dephasing is due to the field inhomogeneities and holds even without any applied gradient pulse ($g = 0$):

$$\Delta\phi_b = \phi_b(\Delta' + \tau) - \phi_b(0), \quad (7)$$

where

$$\phi_b(t) = \gamma \int_t^{t+\tau} b[z(t')] dt' \quad (8)$$

and $\Delta' = 0$ for the PFG-SE sequence. Using the assumption of small τ , we obtain:

$$\phi_b(t) = \gamma\tau b(t). \quad (9)$$

Applying external pulsed gradients g results in an additional phase shift, $\Delta\phi_a$:

$$\Delta\phi_a = \phi_a(t_2) - \phi_a(t_1), \quad (10)$$

where

$$\phi_a(t) = \gamma g \int_t^{t+\delta} z(t') dt'. \quad (11)$$

Considering the above assumption of short τ , we use the following expansion of z :

$$z(t') = z(t) + (t' - t)v_z(t) \quad \text{for } t < t' < t + \delta \quad (12)$$

so that

$$\phi_a(t_1) = k \left[z(t_1) + \frac{\delta}{2} v_z(t_1) \right]$$

and

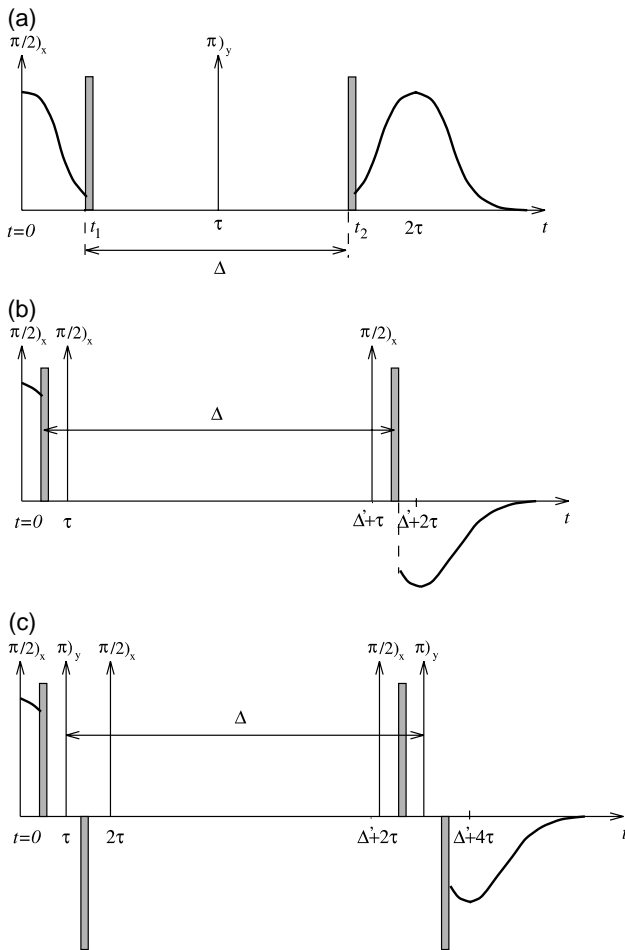


Fig. 1. NMR pulse sequences used in our experiments: we superimpose magnetic field gradient pulses of intensity g and duration δ to a classic spin echo sequence (the shaded rectangles correspond to the magnetic field gradient pulses). (a) PFG-SE sequence; (b) PFG-SSE sequence; (c) APFG-SSE sequence: each gradient pulse has a duration of $\delta/2$, so that the effect of each pair of gradient pulses is equivalent to one pulse of duration δ . The time duration Δ has been chosen here to describe the effective time interval between gradient pulses (or pairs of pulses in the case of APFG-SSE). Δ' is the time duration between $\pi/2_x$ pulses for the PFG-SSE and APFG-SSE sequences.

¹ In practice, such a condition is not very restrictive since, if we need long measurement time, one should use the PFG-SSE sequence and increase the time duration Δ while keeping τ short.

$$\varphi_a(t_2) = k \left[z(t_2) + \frac{\delta}{2} v_z(t_2) \right].$$

Thus

$$\Delta\varphi_a \approx \gamma g \delta \left(\xi + \frac{\delta}{2} \Delta v \right) = k \left(\xi + \frac{\delta}{2} \Delta v \right), \quad (13)$$

$$\Delta\varphi_b \approx \gamma \tau \Delta b,$$

where

$$\Delta u = u(z(t_2)) - u(z(t_1)) \quad \text{for } u = b \text{ or } v \quad (14)$$

and ξ is the particle displacement between t_1 and t_2 ($\xi = z(t_2) - z(t_1)$).

Finally, the total dephasing $\Delta\varphi = \Delta\varphi_a + \Delta\varphi_b$ appears to be a function of the displacement ξ , as expected, and also of the variation of magnetic field Δb and of the variation of velocity Δv :

$$\Delta\varphi = k \left(\xi + \frac{\delta}{2} \Delta v \right) + \gamma \tau \Delta b. \quad (15)$$

The variation of magnetic field, Δb , and of velocity, Δv , depends of course on the displacement ξ of a fluid particle along its trajectory. To characterise the random quantity Δv during the fluid displacement, we introduce the distribution function $p(\Delta v; \xi)$, the probability distribution for a fluid particle to be submitted to a variation of velocity Δv for a displacement ξ . We also introduce the distribution function $p(\Delta b; \Delta v, \xi)$, the probability distribution to observe a variation of magnetic field Δb for a displacement ξ and a variation of velocity Δv .

The magnetisation decay $M(k)/M_0$ can now be expressed as:

$$\langle e^{i\Delta\varphi_j} \rangle = \int \int \int e^{i\Delta\varphi} p(\Delta b; \Delta v, \xi) p(\Delta v; \xi) P_\Delta(\xi) d\Delta b d\Delta v d\xi. \quad (16)$$

We now assume that the variables Δb and Δv corresponding to the variation of b and v for a displacement ξ along Oz are uncorrelated: $\langle \Delta b \Delta v \rangle = 0$. Such an assumption is not easy to justify, but it should be acceptable for an enough random porous matrix. Then, Eq. (16) becomes

$$\langle e^{i\Delta\varphi_j} \rangle = \int \int \int e^{i\Delta\varphi} p(\Delta b; \xi) p(\Delta v; \xi) P_\Delta(\xi) d\Delta b d\Delta v d\xi \quad (17)$$

$p(\Delta b; \xi)$ is the probability distribution for a fluid particle to be submitted to a variation of magnetic field Δb for a displacement ξ .

Introducing $\tilde{p}(\Delta b; \xi)$ (or $\tilde{p}(\Delta v; \xi)$), the Fourier transform of $p(\Delta b; \xi)$ (or $p(\Delta v; \xi)$) relative to Δb (or Δv), we finally obtain

$$\langle e^{i\Delta\varphi_j} \rangle = \int \tilde{p}(\Delta b; \xi) \tilde{p}(\Delta v; \xi) e^{ik\xi} P_\Delta(\xi) d\xi. \quad (18)$$

3. Probability distributions $p(\Delta b; \xi)$ and $p(\Delta v; \xi)$

To make precise the physical meanings of these distributions ($p(\Delta b; \xi)$ and $p(\Delta v; \xi)$), we present the following remarks: the quantity

$$\left(\int p(\Delta b; \xi) P_\Delta(\xi) d\xi \right) d\Delta b$$

represents the fluid particle fraction submitted to a magnetic field variation ranging from Δb to $\Delta b + d\Delta b$. The mean square of the magnetic field variation during the time interval Δ is given by:

$$\langle \Delta b^2 \rangle = \int \left(\int p(\Delta b; \xi) P_\Delta(\xi) d\xi \right) \Delta b^2 d\Delta b.$$

Of course, when the displacement ξ tends to 0, $p(\Delta b; \xi)$ tends to a dirac function: $p(\Delta b; 0) = \delta(\Delta b)$.

On the contrary, when the displacements ξ become much larger than ξ_b , the characteristic length of the variation of b (typically ξ_b is of the order of the grain size), so that b gets uncorrelated with its initial value, $\langle \Delta b^2 \rangle = \langle [b(t_2) - b(t_1)]^2 \rangle$ tends towards the limit value $2\langle b^2 \rangle$. In this last case, $\xi \gg \xi_b$, $p(\Delta b, \xi)$ tends towards

$$\int_{-\infty}^{\infty} p(b) p(b + \Delta b) db,$$

where $p(b)$ is the probability distribution of magnetic field b (this distribution is the resonance spectrum of the fluid protons in the saturated porous medium and it can be derived from the free induction decay). Let us note that except the last point in parentheses, the above remarks also apply to the distribution $p(\Delta v; \xi)$.

As suggested by this discussion, it appears that the behaviour of the distributions $p(\Delta b; \xi)$ and $p(\Delta v; \xi)$ is related to the spatial correlations of the magnetic field fluctuations $b(z)$ and of the velocity fluctuations $v(z)$ for all the fluid particles along their trajectories. Considering now all the fluid particles on their trajectories, the spatial correlation along Oz of the magnetic field deviation $b(z)$ and velocity deviation $v(z)$ are, respectively, defined by the following relations:

$$\theta_b(\xi) = \langle b(0)b(\xi) \rangle, \quad (19)$$

$$\theta_v(\xi) = \langle v(0)v(\xi) \rangle, \quad (20)$$

where $\langle \dots \rangle$ represents an average over all the fluid particles along their trajectories. $\theta_b(\xi)$ and $\theta_v(\xi)$ are decreasing functions of ξ for any random medium.

From these correlation functions, we can derive the width of the distribution $p(\Delta b; \xi)$ and $p(\Delta v, \xi)$. We define $\langle \Delta b^2 \rangle_\xi$ the mean square of the magnetic field shifts associated with a particle displacement ξ in the direction Oz ; $\langle \Delta b^2 \rangle_\xi$ is related to $\theta_b(\xi)$ by

$$\langle \Delta b^2 \rangle_\xi = \langle [b(\xi) - b(0)]^2 \rangle = 2[\theta_b(0) - \theta_b(\xi)]. \quad (21)$$

Similarly, $\langle \Delta v^2 \rangle_\xi$ is defined as the mean square of the velocity variations associated with a displacement ξ and

$$\langle \Delta v^2 \rangle_\xi = \langle [v(\xi) - v(0)]^2 \rangle = 2[\theta_v(0) - \theta_v(\xi)]. \quad (22)$$

4. Application to simple porous medium

Until now, we considered the most general case.

To pursue this discussion, we will consider here the particular case of porous media with a unique length scale l_c , the grain size. Later on we assume that the correlation functions $\theta_b(\xi)$ and $\theta_v(\xi)$ can be approximately represented by the following functions:

$$\begin{aligned} \theta_b(\xi) &= \langle b^2 \rangle \exp\left(-\frac{\xi^\alpha}{\xi_b^\alpha}\right), \\ \theta_v(\xi) &= \langle v^2 \rangle \exp\left(-\frac{\xi^\beta}{\xi_v^\beta}\right). \end{aligned} \quad (23)$$

The characteristic lengths, ξ_b and ξ_v , are expected to be of the order of the grain scale l_c . The exponents α and β depend on the structure of the pore connections and are expected to be of the order unity.

An estimation of $\theta_b(\xi)$ and $\theta_v(\xi)$ can be proposed in the model case where the porous medium is constituted by a randomly oriented channel network. If λ is the individual length of the channels, we find (see Appendix A) that the correlation functions are well represented by the relations (23) with $\xi_b = \xi_v = \lambda/3.5$ and $\alpha = \beta = 1.1$.

From Eqs. (23) and (21), we obtain the mean square of the magnetic field fluctuation for a displacement ξ

$$\langle \Delta b^2 \rangle_\xi = 2 \langle b^2 \rangle \left[1 - \exp\left(-\frac{\xi^\alpha}{\xi_b^\alpha}\right) \right]. \quad (24)$$

Let us remark that this is compatible with the expected limit behaviour for small ξ ($\lim_{\xi \rightarrow 0} \langle \Delta b^2 \rangle_\xi = 0$) and large ξ ($\lim_{\xi \gg \xi_b} \langle \Delta b^2 \rangle_\xi = 2 \langle b^2 \rangle$). The probability distribution of magnetic field b , $p(b)$, can be derived experimentally from the free induction decay; it is presented in Fig. 2

for random monodisperse sphere packings and, as shown, it can be well approximated by a Gaussian distribution. Thus, for large ξ , the distribution $p(\Delta b; \xi)$ is Gaussian. As previously noted, it becomes a Dirac function for small ξ . For intermediate displacement range, we propose as an approximation for $p(\Delta b; \xi)$ the following Gaussian distribution:

$$p(\Delta b; \xi) = \frac{1}{\sqrt{2\pi\sigma_b^2}} \exp\left(-\frac{\Delta b^2}{2\sigma_b^2}\right), \quad (25)$$

where $\sigma_b^2 = \langle \Delta b^2 \rangle_\xi$. This distribution satisfies the expected limit cases ($\xi \rightarrow 0$ and $\xi \rightarrow \infty$).

In the same way, the mean square of the velocity variation is obtained and obeys the expected limit behaviour:

$$\langle \Delta v^2 \rangle = 2 \langle v^2 \rangle \left[1 - \exp\left(-\frac{\xi^\beta}{\xi_v^\beta}\right) \right]. \quad (26)$$

The probability distribution of velocity in the mean flow direction, $p(v_z)$, has been obtained from experiments and numerical simulations [12]; it can be well approximated by an exponential distribution:

$$p(v_z) = \begin{cases} 0 & \text{if } v_z < 0, \\ \frac{1}{\langle v_z \rangle} \exp\left[-\frac{v_z}{\langle v_z \rangle}\right] & \text{if } v_z > 0 \end{cases} \quad (27)$$

with $\langle v_z^2 \rangle = 2 \langle v_z \rangle^2$. While $v = v_z - \langle v_z \rangle$, we obtain:

$$p(v) = \begin{cases} 0 & \text{if } v < -\langle v_z \rangle, \\ \frac{1}{\langle v_z \rangle} \exp\left[-\frac{v + \langle v_z \rangle}{\langle v_z \rangle}\right] & \text{if } v > -\langle v_z \rangle \end{cases} \quad (28)$$

with $\langle v^2 \rangle = \langle v_z \rangle^2$. For large ξ , $p(\Delta v; \xi)$ tends towards

$$\int_{-\infty}^{\infty} p(v) p(v + \Delta v) dv = \frac{1}{2 \langle v_z \rangle} \exp\left(-\frac{|\Delta v|}{\langle v_z \rangle}\right). \quad (29)$$

Thus, we propose to approximate $p(\Delta v; \xi)$ by an exponential distribution

$$p(\Delta v; \xi) = \frac{1}{\sqrt{2}\sigma_v} \exp\left(-\frac{\sqrt{2}|\Delta v|}{\sigma_v}\right), \quad (30)$$

where $\sigma_v^2 = \langle \Delta v^2 \rangle_\xi$.

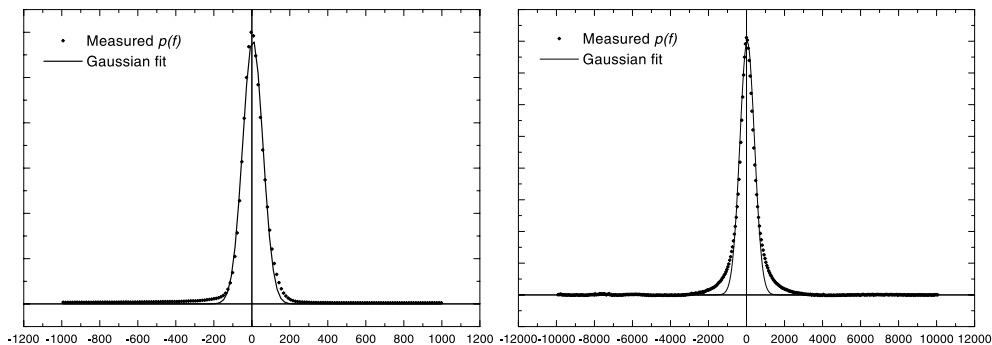


Fig. 2. Resonance frequency spectra $p(f)$ (f in Hz) of water protons for two of our porous samples: packing of glass beads: diameter of 800 μm (left) and 81 μm (right); —: approximation of spectra by Gaussian function.

At this stage, we are able to calculate the Fourier transform $\tilde{p}(\Delta b; \xi)$ and $\tilde{p}(\Delta v; \xi)$

$$\begin{aligned} \tilde{p}(\Delta b; \xi) &= \int e^{i\gamma\tau\Delta b} p(\Delta b; \xi) d\Delta b \\ &= \exp\left(-\frac{\gamma^2\tau^2\sigma_b^2}{2}\right), \end{aligned} \quad (31)$$

$$\tilde{p}(\Delta v; \xi) = \int e^{ik(\delta/2)\Delta v} p(\Delta v; \xi) d\Delta v = \frac{1}{1 + \frac{k^2\delta^2\sigma_v^2}{8}}. \quad (32)$$

We finally obtain the magnetisation decay from Eq. (18)

$$\langle e^{i\Delta\phi_j} \rangle = \int \frac{e^{-\gamma^2\tau^2\langle b^2 \rangle [1 - e^{-(\xi/\xi_b)^\alpha}]} e^{ik\xi} P_\Delta(\xi) d\xi}{1 + \frac{k^2\delta^2\langle v^2 \rangle}{2} [1 - e^{-(\xi/\xi_v)^\beta}]} \quad (33)$$

Some practical consequences of this result will now be discussed in Section 5.

5. Discussion and conclusion

5.1. Effects of the magnetic field inhomogeneities

Let us consider effects of the magnetic field inhomogeneities on the measured magnetisation:

$$\langle e^{i\Delta\phi_j} \rangle = \int e^{-\gamma^2\tau^2\langle b^2 \rangle [1 - e^{-(\xi/\xi_b)^\alpha}]} e^{ik\xi} P_\Delta(\xi) d\xi. \quad (34)$$

These effects are quite easy to estimate: by taking the inverse Fourier transform of $\langle e^{i\Delta\phi_j} \rangle$, we obtain an apparent propagator $P'_\Delta(\xi)$, instead of the correct one $P_\Delta(\xi)$:

$$P'_\Delta(\xi) = \int \langle e^{i\Delta\phi_j} \rangle e^{-ik\xi} dk. \quad (35)$$

The ratio between this apparent propagator and the exact propagator is the correction factor

$$\begin{aligned} f(\xi) &= e^{-\gamma^2\tau^2\langle b^2 \rangle [1 - e^{-(\xi/\xi_b)^\alpha}]} \\ P'_\Delta(\xi) &= e^{-\gamma^2\tau^2\langle b^2 \rangle [1 - e^{-(\xi/\xi_b)^\alpha}]} P_\Delta(\xi). \end{aligned} \quad (36)$$

First, there are simple cases where these effects are easy to discuss: short displacements and long displacements.

5.1.1. Small displacements

If we just consider small displacements (i.e., $\xi \ll \xi_b$), it is obvious that the magnetic field effects will not have to be taken into account. The correction factor will always be very close to 1. Physically, the magnetic field as seen by the fluid particles will not change during the measurement time.

In practice, of course, how small the displacements should be will depend on the parameters and particularly on the frequency bandwidth. This point will be discussed later.

5.1.2. Long displacements

On the opposite, for long displacements ($\xi \gg \xi_b$), the correction factor becomes constant (i.e., independent on the displacement ξ):

$$\lim_{\xi \gg \xi_b} e^{-\gamma^2\tau^2\langle b^2 \rangle [1 - e^{-(\xi/\xi_b)^\alpha}]} = e^{-\gamma^2\tau^2\langle b^2 \rangle}. \quad (37)$$

This behaviour can be physically explained: if a fluid particle population has explored a large enough number of pores, it has also explored all the possible values of the magnetic field fluctuations. Therefore, once this regime is reached, the decay induced will become independent of the displacement. We can remark here that such regimes are not accessible by diffusion experiments because it necessitates very large displacements.

In this case, in theory, the inverse Fourier transform of the magnetisation gives the correct propagator. In practice, we can have serious experimental problems, since $e^{-\gamma^2\tau^2\langle b^2 \rangle}$ could be much smaller than 1 and the signal-to-noise ratio would become very bad. Of course, this will depend on the magnetic field characteristics in the samples, but, because of the magnetic susceptibilities contrasting, porous media are known to make facing this problem difficult.

5.1.3. General case

In practice, there are a lot of cases where we deal with propagator $P_\Delta(\xi)$ for which displacements are neither much smaller nor much larger than the grain size. This is even an objective of interest of PFG NMR experiments to study displacements around the typical grain size and therefore the cases discussed previously cannot be applied.

Thus, we need to look at Eq. (34) in more detail. As previously pointed out, it is easy to measure $\langle b^2 \rangle$ for a given porous medium; the characteristic length ξ_b is expected to be of the order of the grain size and the exponent α of order unity. To obtain approximate values for these parameters, we propose the experiment described in Appendix B; we obtain the following approximations for our bead pack sample: $\alpha \approx 1.6$ and $\xi_b \approx 0.67l_c$. From a general point of view, we do not think that the exact values for these parameters will deeply change our discussions and conclusions.

For our bead pack samples, we measured different values of the frequency bandwidth ($\sqrt{\langle f^2 \rangle} = \gamma\sqrt{\langle b^2 \rangle}/2\pi$) ranging from 52 to 384 Hz for a proton resonance of 100 MHz (2.34 T). Let us remark that such differences in line widths do not result from the difference in bead size but rather from difference in magnetic susceptibilities between bead samples. We can note here that the bandwidth is of the order of 12 Hz for a bulk water sample in our NMR device. These values will now be used as typical frequency bandwidth to draw some practical conclusions.

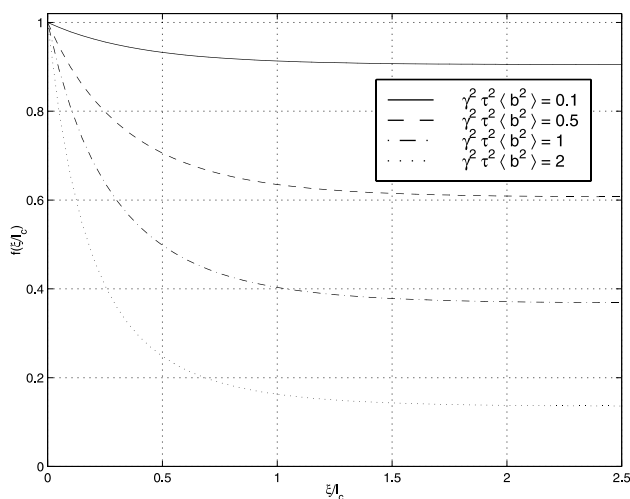


Fig. 3. Correction factor $f(\xi)$ as a function of the reduced displacement ξ for different values of $\gamma^2 \tau^2 \langle b^2 \rangle$.

Small frequency bandwidth. Fig. 3 displays the correction factor $f(\xi)$ as a function of the displacement ξ for different values of $\gamma^2 \tau^2 \langle b^2 \rangle$. We can deduce that in the best case (frequency bandwidth of 52 Hz), the correction factor will stay very close to unity only if the duration τ stays very small, of the order of 1 ms. For example, for $\tau = 1$ ms, the correction factor $f(\xi)$ will vary from 1 to 0.9. This means that we underestimate the weight of large displacements by about 10%. The distortion of the propagator reaches 50% for $\tau = 2.5$ ms.

This is clearly one of the advantages of the PFG stimulated spin echo sequence over the basic PFG spin echo sequence: the PFG-SSE allows one to increase the measurement time while keeping τ small. But in practice, it is very difficult to keep τ as small as 1 ms as τ should be at least a little longer than δ , the gradient pulse duration.

Therefore, such sequences should be used to study the propagator only in very magnetically clean samples. It could also be used if we just consider small displacements. We can now provide an estimation of what we call small displacements here. For a frequency bandwidth of 52 Hz and using a τ duration of 3 ms, the displacements range should stay smaller than one-sixth of the grain size: $\xi < 0.17l_c$.

Large frequency bandwidth. When the frequency bandwidth increases, it appears clearly that such sequences could not be used anymore. Even with a very small τ value such as 1 ms, the correction factor will vary from 1 to 3×10^{-3} for a bandwidth of 384 Hz and the measured propagator $P'_\Delta(\xi)$ will display only very small displacements and hide larger ones.

In this case, even if we try to use Eq. (36), it is impossible to obtain an estimation of the correct propagator; the signal-to-noise ratio will not allow such a correction.

5.1.4. The APFG-SSE sequence

We just discussed the limitations of the basic PFG NMR sequences. When we face large frequency bandwidth, we should use more sophisticated sequences as the APFG-SSE sequence if we wish to perform experiments. The advantages of this sequence have been demonstrated theoretically by Cotts et al. [31] in the case of diffusion in background gradients and the experiments performed by Lucas et al. [32] have illustrated this point in the case of diffusion coefficient imaging.

Let us discuss it in the flow case where the modelling of the magnetic field inhomogeneities by background gradients can no longer be used. Thus, let us go back to the dephasing calculations:

$$\Delta\varphi_b = \varphi_b(t_2) - \varphi_b(t_1). \quad (38)$$

Considering the features of the APFG-SSE sequence, we have in this case:

$$\varphi_b(t) = \int_{t+\tau}^{t+2\tau} \gamma b(t') dt' - \int_t^{t+\tau} \gamma b(t') dt', \quad (39)$$

$$= \gamma \int_t^{t+\tau} [b(t' + \tau) - b(t')] dt'. \quad (40)$$

We still use the approximation of small τ , which is a reasonable assumption for this sequence

$$b(t' + \tau) \approx b(t') + \tau b'(t') \quad (41)$$

so that finally

$$\varphi_b(t) \approx \gamma\tau \int_t^{t+\tau} b'(t') dt', \quad (42)$$

$$\approx \gamma\tau^2 b'(t). \quad (43)$$

Thus, the total dephasing induced by magnetic field inhomogeneities in the case of the APFG-SSE sequence is

$$\Delta\varphi_b \approx \gamma\tau^2 \Delta b'. \quad (44)$$

It now depends on the second-order term of the magnetic field variations while, for the basic sequences, it was depending on the first-order term. This clearly establishes the power of such sequence which cancels the first-order effects.

But unfortunately, it becomes very difficult to give quantitative estimation of this effect. $b'(t)$ is the derivative of $b(t)$ along the fluid particle trajectories

$$b'(t) = \frac{db}{dt} = \frac{db}{dz} \frac{dz}{dt} = g_b v_z, \quad (45)$$

where g_b is the local magnetic field gradient and v_z is the fluid particle velocity along Oz . The probability distribution of this quantity, $g_b v_z$, can neither be experimentally measured nor easily estimated.

We can remark that still using the small τ approximation, the effects of the fluid particle displacement and the velocity variations are not changed by the use of APFG-SSE sequence. This is due to the design of the

sequence where the gradient intensity is inverted after each π_y pulse.

5.2. Effects of the velocity variations

We now consider the effects of the velocity variations on the magnetisation signal

$$\langle e^{i\Delta\phi_j} \rangle = \int \frac{1}{1 + \frac{k^2 \delta^2 \langle v^2 \rangle}{2} [1 - e^{-(\xi/\xi_v)^\beta}]} e^{ik\xi} P_\Delta(\xi) d\xi. \quad (46)$$

This case appears clearly less easy because the correction factor

$$\left\{ 1 + \frac{k^2 \delta^2 \langle v^2 \rangle}{2} [1 - e^{-(\xi/\xi_v)^\beta}] \right\}^{-1}$$

depends now on both the displacement ξ and the wave number k . Let us first discuss simple cases.

5.2.1. Small displacements

Once again, as long as we just consider small displacements (i.e., $\xi \ll \xi_v$), such effects are negligible. This can be directly derived from Eq. (46), but this is also physically obvious: as long as displacements are very much smaller than the grain size, the fluid particle velocities would not change during the measurement time.

In this case, the correct propagator is directly derived from the magnetisation decay by inverse Fourier transform, i.e.,

$$P_\Delta(\xi) = \int \langle e^{i\Delta\phi_j} \rangle e^{-ik\xi} dk. \quad (47)$$

5.2.2. Small velocities or large spacial resolution

Such effects could also be easily neglected if $k^2 \delta^2 \langle v^2 \rangle$ is always much smaller than unity. If k_{\max} is the maximum value for the wave number, we should have

$$k_{\max}^2 \delta^2 \langle v^2 \rangle \ll 1. \quad (48)$$

In practice, the maximum value for the wave number is related to the spatial resolution we wish to obtain for the propagator $P_\Delta(\xi)$ (the spatial resolution is π/k_{\max}).

To obtain microscopic information on the transport process in the porous medium, a typical resolution is one-tenth of the grain size. The corresponding k_{\max} is $10\pi/l_c$

$$k_{\max}^2 \delta^2 \langle v^2 \rangle \approx 100\pi^2 \frac{\delta^2 \langle v^2 \rangle}{l_c^2} \quad (49)$$

and the condition $k_{\max}^2 \delta^2 \langle v^2 \rangle \ll 1$ becomes

$$\delta^2 \langle v^2 \rangle \ll \frac{l_c^2}{100\pi^2}. \quad (50)$$

A trivial and necessary condition would be that the typical displacement during the gradient pulse should be much smaller than the grain size, but this does not seem to be sufficient.

Let us examine such a condition for typical values of the experimental parameters: $\delta \sim 1$ ms, $\sqrt{\langle v^2 \rangle} \sim 1$ mm/s, and $l_c \sim 100 \mu\text{m}$; the condition (50) is not satisfied. Furthermore, we can notice that it is not for the PFG NMR experiments we made and also for those published by different authors (in cases where we can obtain the experimental parameters).

We can remark that the condition (48) can be physically interpreted: the typical displacement during the gradient pulse should be much smaller than the spatial resolution of the measured propagator, but the introduction of the grain size in this discussion appears to us more relevant.

5.2.3. General case

When the previous conditions are not met, we have to consider Eq. (46) in more detail; while the correction factor depends on both k and ξ , the operation described by this equation is no more a Fourier transform. Furthermore, in this case, there is not an easy way to derive $P_\Delta(\xi)$ from the magnetisation decay.

At this stage, our question is mainly: if we do not satisfy the previous conditions, how important could be the errors on the propagator? Thus, our goal is not to provide an exact and detailed mathematical analysis of Eq. (46), but to find a way to get an estimation of the correction factor effects. We describe in Appendix C the process used to obtain an estimation of the propagator from Eq. (46).

Using such an approximation, we verify the effects on one of our experiments: in this case, we have $k_{\max}^2 \delta^2 \langle v^2 \rangle \approx 4.8$, $\delta \sqrt{\langle v^2 \rangle} \approx 7.5 \mu\text{m}$, and $l_c \approx 145 \mu\text{m}$. The required conditions are not satisfied, but we can observe in Fig. 4 that the original propagator (i.e., ob-

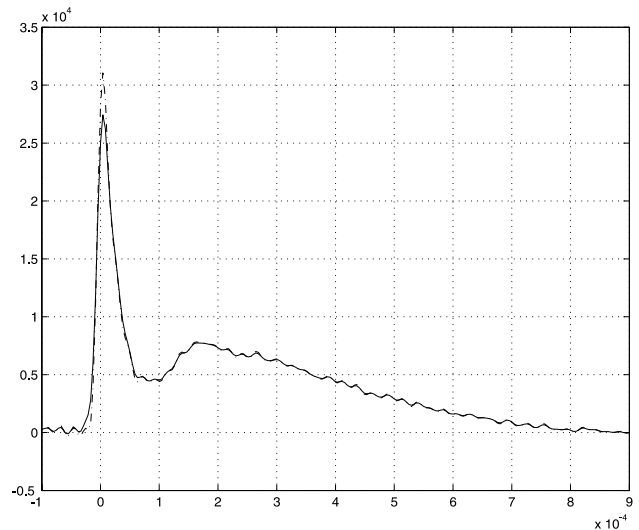


Fig. 4. Propagator $P_\Delta(\xi)$ (m^{-1}) as a function of ξ (m); comparison between the measured propagator (—), and the corrected propagator (---); the corrected propagator was deduced from the measured one taking account the velocity variations effects.

tained without taking into account the velocity variation effects) and the corrected propagator are very close. We verified these features for all our experiments and we always observed the same result: the differences are still very small and sometimes unobservable.

Why do the effects appear so small when the necessary conditions are not satisfied? A rigorous answer is not straightforward. We can remark that Eq. (50) is very conservative: it guarantees that for every wave number value ranging from 0 to k_{\max} , the correction factor will be negligible. In practice, even if the condition is not satisfied, the correction factor will stay very close to 1 on the most part of the wave number range, so that after integration, the effects will stay very limited.

5.2.4. Conclusion

We can try to draw practical conclusions from this study. We just verified that, when conservative and rigorous conditions are not satisfied, the errors on the propagator measurements may stay small. Thus, we try to establish a practical condition that could allow one to neglect the velocity effects on measured propagator.

In our case, $\delta\sqrt{\langle v^2 \rangle}/l_c \approx 0.052$; we have tested the effects on the measured propagator when we increase this parameter (for example, by increasing δ while keeping everything else unchanged; in particular, this implies decreasing the gradient intensities so that k values do not change). From the correct propagator, we use Eq. (46) to construct the magnetisation decay and, then, we compute the Fourier transform. We present in Fig. 5 the results for three values of the ratio $\delta\sqrt{\langle v^2 \rangle}/l_c$: 0.052, 0.2, and 0.5.

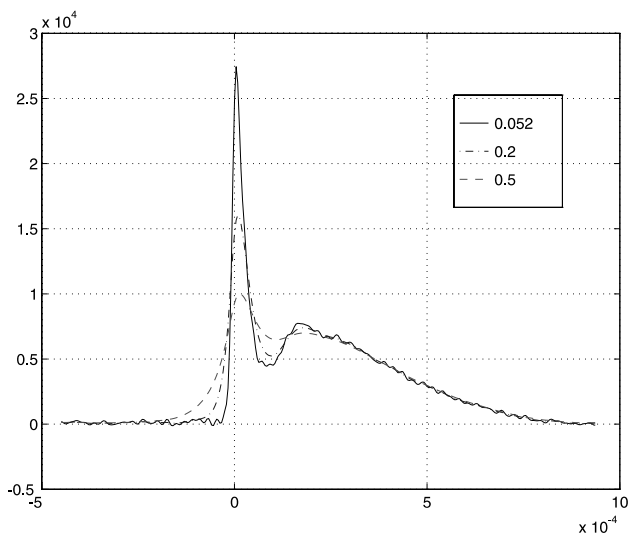


Fig. 5. Propagator $P_A(\xi)$ (m^{-1}) as a function of ξ (m); effects on the measured propagator of the velocity variations for different values of the ratio $\delta\sqrt{\langle v^2 \rangle}/l_c$ (—: $\delta\sqrt{\langle v^2 \rangle}/l_c = 0.052$; ---: $\delta\sqrt{\langle v^2 \rangle}/l_c = 0.2$; -·-: $\delta\sqrt{\langle v^2 \rangle}/l_c = 0.5$).

Therefore, it appears that as long as $\delta\sqrt{\langle v^2 \rangle}/l_c < 0.1$ the errors on the propagator stay small. We find very similar results for all other experiments, so that we can propose the following condition:

$$\frac{\delta\sqrt{\langle v^2 \rangle}}{l_c} \ll 1. \quad (51)$$

6. Conclusion

In this work, we studied in detail some of the errors that could be made when performing PFG NMR experiments on porous media flows. We propose a statistical model based on spatial correlations of the velocity field and the magnetic field to describe their effects on the measurements.

We are aware that the choices we made for the spatial autocorrelation functions of b and v are necessarily arbitrary: we assumed that these functions could be well represented by stretched exponential functions. As long as such an assumption can be made for a given porous medium, the model we presented here stays valid. We have verified that different values for the correlation parameters (α , β , ξ_b , or ξ_v) do not change our conclusions (of course, as long as these parameters stay in a range where they keep a physical meaning).

We explained quantitatively why basic PFG NMR sequences are very limited when used to study flows through porous media. From the magnetic properties of the medium and the analysis we performed in this paper, we can easily predict when these sequences will fail. In such cases, we should use the APFG-SSE sequence; on a theoretical point of view, we can conclude that this sequence is clearly better, but, in this case, quantitative predictions cannot be provided.

We also discussed the effects of the finite gradient pulse duration on the measured propagator: in addition to the particle displacements, phase shifts also encode velocity variations during the measurement time. We analysed in detail this effect and we finally propose a practical condition that allows one to neglect it: the mean displacement during the gradient pulse should stay lower than the typical grain size.

This study clearly demonstrates the advantage in using strong gradient pulses: this allows one to keep the gradient pulse duration δ short for a given value of the wave number k : short δ values minimize the effects of the velocity variation. It also allows one to keep τ duration short and this finally minimizes the effects of the magnetic field inhomogeneities.

We described here effects induced by the flow through the porous matrix and we considered a porous medium with a well-defined length scale. For a porous medium with wide ranges of length scales, only the scale

corresponding to the backbone of the flow will be relevant. For example, let us consider the case of a porous medium with two length scales: a micro porosity domain and a macro porosity domain; the magnetisation of the fluid part enclosed in a micro porosity domain will not be described by our model because transport is dominated by diffusion. For the macro porosity domain, where the fluid flows, our model will be relevant. From a general point of view, the most conservative forms of the validity conditions should stay valid without any length scale consideration ($\gamma^2 \tau^2 \langle b^2 \rangle \ll 1$ for the PFG NMR and PFG-SSE sequences and $k_{\max}^2 \delta^2 \langle v^2 \rangle < 10$) so that most of our conclusions stay valid.

We finally conclude that, in practical terms, PFG NMR measurements of flow through porous media can be correctly performed; PFG NMR was shown to be a relevant tool to investigate transport and structure at the pore scale. We provided here some elements to help facing artefacts that can distort measurements. We just want to point out that it is important to check such experiments by comparing the flow mean velocity obtained from NMR measurement with the one deduced from the global flow rate through the sample: this can help to detect artefacts.

Appendix A

Let us consider a porous medium constituted by a network of randomly oriented connected channels and assume that:

- All the channels are cylindrical and identical with a length λ .
- The network is statistically homogeneous and isotropic; $f(\Omega)$ the orientation probability distribution of the channels is constant and uniform.
- On a particle trajectory T_j , the values of b and v are constant in a particular channel, but different and uncorrelated in different channels. It follows that:

$$\frac{\theta_v(\xi)}{\langle v^2 \rangle} = \frac{\theta_b(\xi)}{\langle b^2 \rangle} = h(\xi), \quad (\text{A.1})$$

where $h(\xi)$ is the normalised correlation function.

Let us now consider now all the channels with an orientation of Ω and note $g(\Omega, \xi)$ the normalised correlation function associated to this orientation:

$$h(\Omega, \xi) = \begin{cases} 0 & \text{if } \xi > \lambda \cos \Theta, \\ 1 - \frac{\xi}{\lambda \cos \Theta} & \text{if } 0 < \xi < \lambda \cos \Theta, \end{cases} \quad (\text{A.2})$$

where Θ is the angle (Ω, Oz) . In the first case, all particles have left their channels; the second part corresponds to the particle fraction still in their channels for a displacement ξ along the direction Oz . Consequently

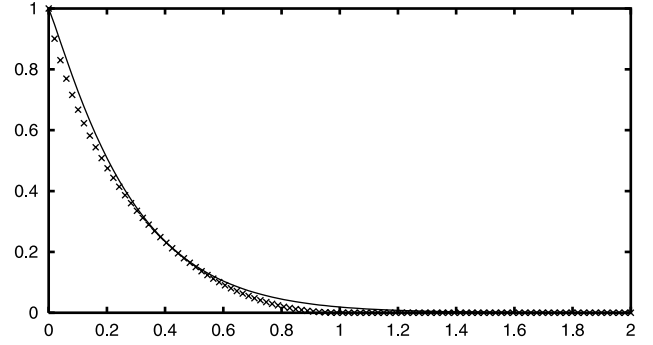


Fig. 6. Normalised correlation function $h(\xi/\lambda)$ calculated (\times) for a model porous medium constituted by a network of randomly oriented connected channels. —: approximation by a stretched exponential function $\exp(-3.5\xi/\lambda)^{1.1}$.

$$h(\xi) = \int h(\Omega, \xi) f(\Omega) d\Omega \quad (\text{A.3})$$

$$= \int_{0 < \xi < \lambda \cos \Theta} \left(1 - \frac{\xi}{\lambda \cos \Theta} \right) \sin \Theta d\Theta \quad (\text{A.4})$$

$$= \int_0^{\Theta_c} \left(1 - \frac{\xi}{\lambda \cos \Theta} \right) \sin \Theta d\Theta, \quad (\text{A.5})$$

where $\Theta_c = \arccos(\xi/\lambda)$. Finally, one obtains:

$$h(\xi) = \begin{cases} 0 & \text{if } \xi > \lambda, \\ 1 - \frac{\xi}{\lambda} (1 - \ln \frac{\xi}{\lambda}) & \text{if } 0 < \xi < \lambda. \end{cases} \quad (\text{A.6})$$

This function, presented in Fig. 6, is correctly fitted by $\exp(-3.5\xi/\lambda)^{1.1}$.

Appendix B

We can remark that even in the absence of any applied gradient ($k = 0$), magnetic field inhomogeneities will induce a magnetisation decay as long as the fluid particles are travelling:

$$\langle e^{i\Delta\phi_j} \rangle = \int e^{-\gamma^2 \tau^2 \langle b^2 \rangle [1 - e^{-(\xi/\xi_b)^2}] P_\Delta(\xi)} d\xi. \quad (\text{B.1})$$

The magnetisation decay can be measured as a function of τ : $E(\tau) = \langle e^{i\Delta\phi_j} \rangle$. If we know the propagator $P_\Delta(\xi)$, we can use Eq. (B.1) to find the best values of α and ξ_b . If we use very very short measurement time corresponding to very small displacement, the propagator corresponds to the velocity probability distribution as it can be derived from numerical simulation.

Using the simplest PFG NMR sequence, we measure the magnetisation as a function of τ . We limited the measurement time (2τ), so that displacements stay very short and the fluid particles keep the same velocity; in this case, $\xi = 2\tau v_z$ and the propagator is directly related to the velocity probability distribution

$$P_{2\tau}(\xi) = \frac{p(v_z)}{2\tau}. \quad (\text{B.2})$$

Finally, Eq. (B.1) becomes

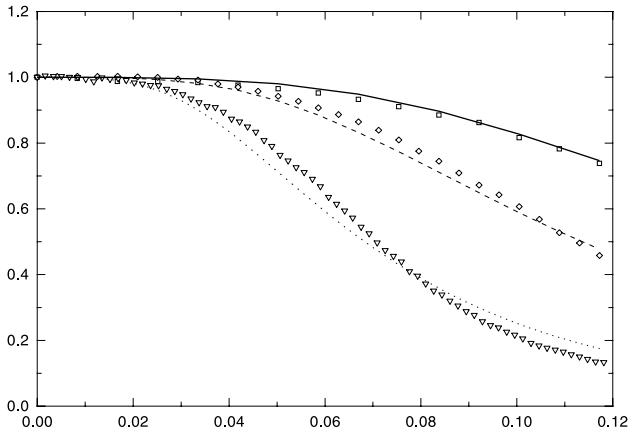


Fig. 7. Decay of the magnetisation $E(\tau)$ as a function of the mean displacement $\langle \xi \rangle / l_c$ for different mean velocities; measurements (lines), and calculations (symbols); — and \square : $\langle v_z \rangle = 6.70$ mm/s; -- and \diamond : $\langle v_z \rangle = 3.35$ mm/s; \cdots and ∇ : $\langle v_z \rangle = 1.34$ mm/s.

$$E(\tau) = \int e^{-\gamma^2 \tau^2 \langle b^2 \rangle [1 - e^{-(2\tau v_z / \xi_b)^2}] } p(v_z) dv_z. \quad (\text{B.3})$$

To a given τ value corresponds a mean displacement $\langle \xi \rangle = 2\tau \langle v_z \rangle$.

We measured $E(\tau)$ for one of our samples (800 μm bead pack) for different mean velocities; we compute the right-hand side of Eq. (B.3) by varying the values of α and ξ_b to reproduce the experimental decay $E(\tau)$. Fig. 7 displays the measurement and the curves obtained from Eq. (B.3) as a function of $\langle \xi \rangle / l_c = 2\tau \langle v_z \rangle / l_c$; we finally obtain the following approximations: $\alpha \approx 1.6$ and $\xi_b \approx 0.67 l_c$.

Appendix C

We consider Eq. (46); let us call $E(k)$ the magnetisation decay measured from PFG NMR experiments: $E(k) = \langle e^{i\Delta\varphi_i} \rangle$. We obtain:

$$E(k) \left[1 + \frac{k^2 \delta^2 \langle v^2 \rangle}{2} \right] = \int P_\Delta(\xi) e^{ik\xi} d\xi + \int P_\Delta(\xi) K(k, \xi) e^{ik\xi} d\xi, \quad (\text{C.1})$$

where the function $K(k, \xi)$ is

$$K(k, \xi) = \frac{k^2 \delta^2 \langle v^2 \rangle e^{-|\xi/\xi_v|^\beta}}{2 + k^2 \delta^2 \langle v^2 \rangle (1 - e^{-|\xi/\xi_v|^\beta})}. \quad (\text{C.2})$$

Let us remark that $\int P_\Delta(\xi) K(k, \xi) e^{ik\xi} d\xi$ depends only on k ; taking the inverse Fourier transform of Eq. (C.1), we now obtain:

$$P_\Delta(\xi) = \int E(k) \left[1 + \frac{k^2 \delta^2 \langle v^2 \rangle}{2} \right] e^{-ik\xi} dk - \int \left[\int P_\Delta(\xi) K(k, \xi) e^{ik\xi} d\xi \right] e^{-ik\xi} dk. \quad (\text{C.3})$$

To obtain an estimation of $P_\Delta(\xi)$, we construct the following series from Eq. (C.3):

$$p_0(\xi) = \int E(k) \left[1 + \frac{k^2 \delta^2 \langle v^2 \rangle}{2} \right] e^{-ik\xi} dk, \\ p_{n+1}(\xi) = p_0(\xi) - \int \left[\int p_n(\xi) K(k, \xi) e^{ik\xi} d\xi \right] e^{-ik\xi} dk. \quad (\text{C.4})$$

This series converges very quickly and we assume that we obtain a good approximation for the corrected propagator $P_\Delta(\xi)$ as given by Eq. (46).

References

- [1] K.R. Brownstein, C.E. Tarr, Importance of classical diffusion in NMR studies of water in biological cells, *Phys. Rev. A* 19 (1979) 2246–2253.
- [2] W.E. Kenyon, J.J. Howard, A. Sezginer, C. Straley, A. Matteson, Horkowitz, R. Ehrlich, Pore-size distributions and NMR in microporous cherty sandstones, *Transactions of the SPLWA Thirtieth Annual Logging Symposium*, 1989.
- [3] S. Torquato, M. Avellanda, Diffusion and reaction in heterogeneous media: pore size distribution, relaxation time and mean survival time, *J. Chem. Phys.* 95 (1991) 6477–6489.
- [4] R.L. Kleinberg, S.A. Horsfield, T_1/T_2 ratio and frequency dependence of NMR relaxation in porous sedimentary rocks, *J. Colloid Interface Sci.* 158 (1993) 195–198.
- [5] P.D. Majors, J.L. Smith, F.S. Kovarik, E. Fukushima, NMR spectroscopic imaging of oil displacement in dolomite, *J. Magn. Reson.* 89 (1990) 470–478.
- [6] G. Guillot, G. Kassab, J.P. Hulin, P. Rigord, Monitoring of tracer dispersion in porous media by NMR imaging, *J. Phys. D: Appl. Phys.* 24 (1991) 763–773.
- [7] D.G. Cory, N. Garroway, Measurement of translational displacement probabilities by NMR: an indicator of compartmentation, *Magn. Reson. Med.* 14 (1990) 435–444.
- [8] P.T. Callaghan, D. MacGowan, K.J. Packer, F.O. Zeleza, Diffraction like effects in NMR diffusion studies of fluids in porous media, *Nature* (1991) 467–468.
- [9] P.P. Mitra, P.N. Sen, L.M. Schwartz, P. LeDoussal, Diffusion propagator as a probe of the structure of porous media, *Phys. Rev. Lett.* 65 (1993) 3555–3558.
- [10] M.D. Hürlimann, L.L. Latour, C.H. Sotak, Diffusion measurement in sandstone core: NMR determination of surface-to-volume ratio and surface relaxivity, *Magn. Reson. Imaging* (1994) 325–327.
- [11] T.M. De Swiet, P.N. Sen, Decay of nuclear magnetization by bounded diffusion in a constant field gradient, *J. Chem. Phys.* 100 (1994) 5597–5604.
- [12] L. Lebon, L. Oger, J. Leblond, J.P. Hulin, N.S. Martys, L.M. Schwartz, Pulsed gradient NMR measurements and numerical simulation of flow velocity distribution in sphere packings, *Phys. Fluids* 8 (1996) 293–301.
- [13] Y.E. Kutsovsky, L.E. Scriven, H.T. Davis, B.E. Hammer, NMR imaging of velocity profiles and velocity distributions in bead packs, *Phys. Fluids* 8 (1996) 863–871.
- [14] A. Ding, D. Candela, Probing nonlocal tracer dispersion in flows through random porous media, *Phys. Rev. B* 54 (1996) 656–660.
- [15] J.D. Seymour, P.T. Callaghan, “Flow-diffraction” structural characterization and measurement of hydrodynamic dispersion

- in porous media by PGSE NMR, *J. Magn. Res., Ser. A* 122 (1996) 90–93.
- [16] K.J. Packer, J.J. Tessier, The characterization of fluid transport in a porous solid by pulsed gradient stimulated echo NMR, *Mol. Phys.* 87 (1996) 267–272.
- [17] L. Lebon, J. Leblond, J.P. Hulin, Experimental measurement of dispersion at short times using a pulsed field gradient NMR technique, *Phys. Fluids* 9 (1997) 481–490.
- [18] S. Stapf, K.J. Packer, R.G. Graham, J.-F. Thovert, P.M. Adler, Spatial correlation and dispersion for fluid transport through packed glass beads studied by pulsed field-gradient NMR, *Phys. Rev. E* 58 (1998) 6206–6221.
- [19] P.T. Callaghan, *Principles of Nuclear Magnetic Resonance Microscopy*, Clarendon Press, Oxford, 1991.
- [20] E.L. Hahn, Spin echoes, *Phys. Rev.* 15 (1950) 580–594.
- [21] H.C. Torrey, Bloch equations with diffusion terms, *Phys. Rev.* 104 (1956) 563–565.
- [22] C.H. Neuman, Spin echo of spins diffusing in a bounded medium, *J. Chem. Phys.* 60 (1974) 4508–4511.
- [23] J.C. Tarczón, W.P. Halperin, Interpretation of NMR diffusion measurements in uniform- and nonuniform-field profiles, *Phys. Rev. B* 32 (1985) 2798–2807.
- [24] P. Hardy, M. Henkelman, On the transverse relaxation rate enhancement induced by diffusion of spins through inhomogeneous fields, *Magn. Reson. Med.* 17 (1991) 348–356.
- [25] P. Le Doussal, P.N. Sen, Decay of nuclear magnetization by diffusion in a parabolic magnetic field: an exact solvable model, *Phys. Rev. B* 46 (1992) 3465–3485.
- [26] R.J.S. Brown, P. Fantazzini, Condition for initial quasilinear T_2^{-1} versus τ for Carr–Purcell–Meiboom–Gill NMR with diffusion and susceptibility differences in porous media and tissues, *Phys. Rev. B* 47 (1993) 14823–14834.
- [27] P.P. Mitra, P. Le Doussal, Long-time magnetization relaxation of spins diffusing in a random field, *Phys. Rev. B* 44 (1991) 12035–12038.
- [28] N.F. Fatkuilin, Spin relaxation and diffusional damping of the spin-echo amplitude of a particle moving in a random Gaussian magnetic field, *Sov. Phys. JETP* 74 (1992) 833–838.
- [29] E.O. Stejskal, J.E. Tanner, Spin diffusion measurements: spin echoes in the presence of a time-dependent field gradient, *J. Chem. Phys.* 42 (1965) 288–292.
- [30] J.E. Tanner, Use of the stimulated echo in NMR diffusion studies, *J. Chem. Phys.* 52 (1970) 2523–2526.
- [31] R.M. Cotts, M.J.R. Hoch, T. Sun, J.T. Marker, Pulsed field gradient stimulated echo methods for improved NMR diffusion measurements in heterogeneous systems, *J. Magn. Reson.* 83 (1989) 252–266.
- [32] A.J. Lucas, S.J. Gibbs, E.W.G. Jones, M. Peyron, A.D. Derbyshire, L.D. Hall, Diffusion imaging in the presence of static magnetic-field gradients, *J. Magn. Reson.* 104 (1993) 273–282.